

## Compositional dependence of the bowing parameter for the direct and indirect band gaps in Ge<sub>1-y</sub>Sn<sub>y</sub> alloys

J. D. Gallagher, C. L. Senaratne, J. Kouvetakis, and J. Menéndez

Citation: [Applied Physics Letters](#) **105**, 142102 (2014); doi: 10.1063/1.4897272

View online: <http://dx.doi.org/10.1063/1.4897272>

View Table of Contents: <http://scitation.aip.org/content/aip/journal/apl/105/14?ver=pdfcov>

Published by the [AIP Publishing](#)

---

### Articles you may be interested in

[Indirect-to-direct band gap transition in relaxed and strained Ge<sub>1-x-y</sub>Si<sub>x</sub>Sn<sub>y</sub> ternary alloys](#)

J. Appl. Phys. **116**, 063712 (2014); 10.1063/1.4889926

[Fundamental band gap and direct-indirect crossover in Ge<sub>1-x-y</sub>Si<sub>x</sub>Sn<sub>y</sub> alloys](#)

Appl. Phys. Lett. **103**, 202104 (2013); 10.1063/1.4829621

[Pseudomorphic GeSn/Ge\(001\) quantum wells: Examining indirect band gap bowing](#)

Appl. Phys. Lett. **103**, 032106 (2013); 10.1063/1.4813913

[Investigation of the direct band gaps in Ge<sub>1-x</sub>Sn<sub>x</sub> alloys with strain control by photoreflectance spectroscopy](#)

Appl. Phys. Lett. **100**, 102109 (2012); 10.1063/1.3692735

[High carrier concentration induced effects on the bowing parameter and the temperature dependence of the band gap of GaIn<sub>1-x</sub>N](#)

J. Appl. Phys. **110**, 103506 (2011); 10.1063/1.3660692

---

The advertisement features a red and white color scheme. On the left, text reads 'Confidently measure down to 0.01 fA and up to 10 PΩ' and 'Keysight B2980A Series Picoammeters/Electrometers'. A red button with white text says 'View video demo >'. On the right, there is an image of the Keysight B2980A device and the Keysight Technologies logo.

## Compositional dependence of the bowing parameter for the direct and indirect band gaps in $\text{Ge}_{1-y}\text{Sn}_y$ alloys

J. D. Gallagher,<sup>1</sup> C. L. Senaratne,<sup>2</sup> J. Kouvetakis,<sup>2</sup> and J. Menéndez<sup>1</sup>

<sup>1</sup>Department of Physics, Arizona State University, Tempe, Arizona 85287-1504, USA

<sup>2</sup>Department of Chemistry and Biochemistry, Arizona State University, Tempe, Arizona 85287-1604, USA

(Received 4 September 2014; accepted 19 September 2014; published online 8 October 2014)

Photoluminescence spectroscopy has been used to determine the direct gap  $E_0$  of  $\text{Ge}_{1-y}\text{Sn}_y$  alloys over a broad compositional range from pure Ge to Sn concentrations exceeding 10%. A fit of the compositional dependence of  $E_0$  using a standard quadratic expression is not fully satisfactory, revealing that the bowing parameter (quadratic coefficient)  $b_0$  is compositionally dependent. Excellent agreement with the data is obtained with  $b_0(y) = (2.66 \pm 0.09) \text{ eV} - (5.4 \pm 1.1)y \text{ eV}$ . A theoretical model of the bowing is presented, which explains the strong compositional dependence of the bowing parameter and suggest a similar behavior for the indirect gap. Combining the model predictions with experimental data for samples with  $y \leq 0.06$ , it is proposed that the bowing parameter for the indirect gap is  $b_{\text{ind}}(y) = (1.11 \pm 0.07) \text{ eV} - (0.78 \pm 0.05)y \text{ eV}$ . The compositional dependence of the bowing parameters shifts the crossover concentration from indirect to direct gap behavior to  $y_c = 0.087$ , significantly higher than the value predicted earlier based on strictly quadratic fits. © 2014 AIP Publishing LLC. [<http://dx.doi.org/10.1063/1.4897272>]

Non-linearities in the compositional dependence of optical transition energies in alloy semiconductors are usually described by a quadratic expression whose proportionality constant is known as the bowing parameter  $b$ . Deviations from such quadratic dependence are in most cases modest and have only been unambiguously demonstrated in a few alloy systems.<sup>1,2</sup> A notable exception are nitride semiconductors with  $\text{AB}_{1-x}\text{N}_x$  stoichiometries,<sup>3,4</sup> which display a giant, non-constant bowing parameter as a result of wave function localization.<sup>5-8</sup> In the case of group-IV alloys, the prototypical  $\text{Si}_{1-x}\text{Ge}_x$  system is characterized by very small  $b$ 's,<sup>9</sup> but significantly larger bowings have been reported for the analogous  $\text{Ge}_{1-y}\text{Sn}_y$  alloy.<sup>9</sup> This system is therefore more attractive from the point of view of studying possible deviations from the standard quadratic formulas. Such studies are very important from a practical perspective because the bowing parameters  $b_0$  and  $b_{\text{ind}}$  for the lowest direct ( $E_0$ ) and indirect ( $E_{\text{ind}}$ ) transitions have a substantial influence on the predicted crossover concentration  $y_c$  from indirect- to direct-gap semiconductor. Whereas a linear interpolation between Ge and  $\alpha$ -Sn suggest  $y_c = 0.2$ , in agreement with theoretical calculations within the Virtual Crystal Approximation (VCA),<sup>10-12</sup> experimental results indicate that the crossover occurs at much lower Sn concentrations. For example, extrapolating room temperature photoluminescence (PL) results from samples with  $y \leq 0.06$ , Jiang *et al.* predict  $y_c = 0.073$ .<sup>13</sup> The substantial difference with the VCA result is due to the fact that  $b_0 > b_{\text{ind}}$ . It is therefore apparent that any compositional dependence of these parameters could change the predicted crossover composition in a significant way. Due to the small compositional range probed in Ref. 13, such effects could not be observed. Excellent fits were obtained by assuming  $b_0$  and  $b_{\text{ind}}$  to be constants. In this letter, however, we report PL experiments from samples with a wider range of Sn concentrations exceeding  $y = 0.10$ . The extended data set shows compelling evidence that  $b_0$  is

not constant. The implications of this finding for the predicted crossover concentration  $y_c$  are discussed in detail.

Thick, luminescent  $\text{Ge}_{1-y}\text{Sn}_y$  films were grown on Ge-buffered Si by Ultra-High Vacuum Chemical Vapor Deposition (UHV-CVD) of  $\text{Ge}_3\text{H}_8$  and  $\text{SnD}_4$ . Growth details were reported in Refs. 13 and 14. The Sn concentrations were determined from Rutherford Backscattering (RBS) and X-ray diffraction. The agreement between the two techniques is excellent. PL experiments were performed at room temperature in samples excited with 200 mW of 980 nm radiation. The wide compositional range requires the use of three detectors: a liquid-nitrogen cooled InGaAs diode (up to 2300 nm), a thermoelectrically cooled InGaAs device (up to 2500 nm), and a PbS detector (beyond 2500 nm). The system response with the three detectors was calibrated with a tungsten-halogen lamp and the spectral energy accuracy was verified by measuring the emission lines from an argon-arc lamp.

The PL spectrum of  $\text{Ge}_{1-y}\text{Sn}_y$  is characterized by a strong peak associated with  $E_0$  and a weaker peak assigned to  $E_{\text{ind}}$ . The direct gap  $E_0$  corresponds to transitions between the local minimum of the conduction band (CB) and the absolute maximum of the valence band (VB) at the center of the Brillouin zone (BZ). We denote these states as  $\Gamma_c$  and  $\Gamma_v$ , respectively. The indirect gap  $E_{\text{ind}}$  corresponds to transitions between  $\Gamma_v$  and the absolute minimum of the CB at the  $L$  point of the BZ. This state is denoted as  $L_c$ .  $E_0$  emission is initially modeled as an exponentially modified Gaussian (EMG), whereas  $E_{\text{ind}}$  emission is modeled as a Gaussian. In a second step, the EMG is fit with a generalized van Roosbroeck-Shockley expression that accounts for strain and excitonic effects. The main adjustable parameter of this expression is  $E_0$ . The indirect gap  $E_{\text{ind}}$  is obtained by subtracting 31 meV from the peak energy of the Gaussian lineshape associated with the indirect emission. A full account of the methodology used to adjust the band gaps is given in

Ref. 13. At low Sn-concentrations the peaks are well separated, but they approach each other as the Sn concentration is increased and can no longer be distinguished for  $y > 0.06$ . This is illustrated in Fig. 1, which shows spectra from samples in the vicinity of  $y = 0.05$ —where the indirect gap emission is barely distinguishable as a shoulder on the low-energy side of the stronger  $E_0$  peak—and spectra for samples with  $y = 0.075/0.080$  in which only a single peak is observed.

Figure 2 shows the  $E_0$  and  $E_{\text{ind}}$  energies determined from the above fits, including data points from Ref. 13. The compositional dependence of optical transition energies is usually written as a quadratic expression which in the case of  $\text{Ge}_{1-y}\text{Sn}_y$  alloys takes the form  $E_{\text{cv}}(y) = E_{\text{cv}}^{\text{Ge}}(1-y) + E_{\text{cv}}^{\text{Sn}}y - b_{\text{cv}}y(1-y)$ . At the simplest level of theory, the shift is obtained from a perturbation to the VCA transition energies, and the bowing parameter is given by<sup>15</sup>

$$b_{\text{cv}} = -|M(y)|^2 [F(E_c, y) - F(E_v, y)], \quad (1)$$

where  $M(y)$  is a matrix element arising from the potential difference between the actual alloy and the VCA alloy. The function  $F(E, y)$  is

$$F(E, y) = \frac{1}{\Omega^2(y)} \wp \int dE' \frac{\rho_{\text{at}}(E', y)}{E - E'}, \quad (2)$$

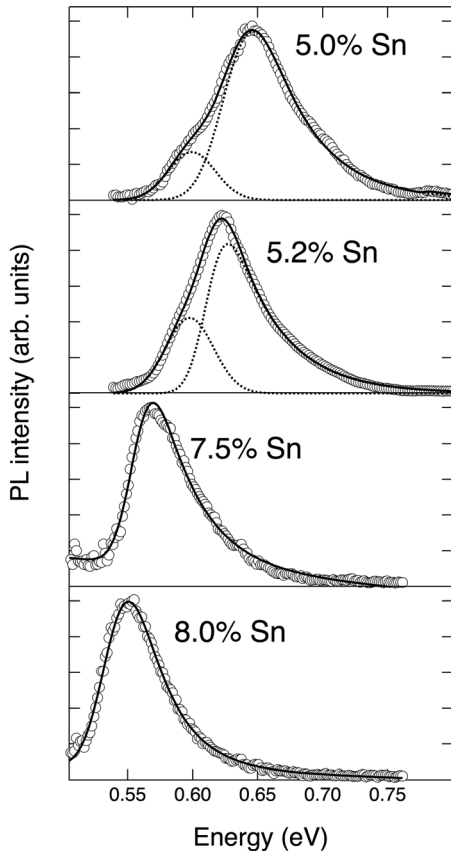


FIG. 1. Room temperature photoluminescence spectrum from selected  $\text{Ge}_{1-y}\text{Sn}_y$  films. The solid lines represent theoretical fits, either by assuming a single contribution (lower two panels) or separate contributions from the direct and indirect band gaps (top two panels). In the later case, the two contributions are shown as dotted lines.

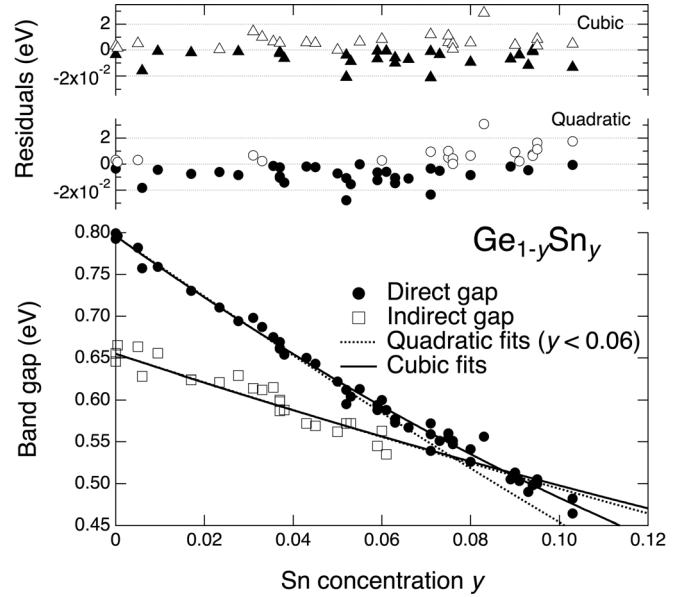


FIG. 2. Direct and indirect band gap energies extracted from room-temperature photoluminescence experiments. The dotted lines are the quadratic fits for  $y < 0.06$ . The solid lines represent the cubic fits, as discussed in the text. The upper panels show the residuals for fits of the direct gap energy with the cubic expression and with a quadratic expression over the entire compositional range. Black (white) markers correspond to negative (positive) residuals.

where  $\Omega(y)$  is the volume of the unit cell of the virtual crystal and  $\rho_{\text{at}}(E', y)$  is the VCA electronic density of states (DOS) (in states per atom per unit of energy). The symbol  $\wp$  denotes a principal part integration.  $F(E, y)$  is in general a function of  $y$ , so that even under the crude assumption  $|M| = \text{constant}$ ,<sup>15</sup> the bowing parameter  $b_{\text{cv}}$  becomes a function of composition. In previous work on  $\text{Ge}_{1-y}\text{Sn}_y$  alloys, however, the number of data points and/or the compositional range explored was too small to detect any possible compositional dependence in the bowing parameters  $b_0$  and  $b_{\text{ind}}$ . In Ref. 13, for example, excellent agreement with experiment was found using constant  $b_0 = 2.46 \pm 0.06$  eV and  $b_{\text{ind}} = 1.03 \pm 0.11$  eV. (The end values were taken as  $E_0^{\text{Ge}} = 0.796$  eV,  $E_0^{\text{Sn}} = -0.413$  eV,  $E_{\text{ind}}^{\text{Ge}} = 0.655$  eV, and  $E_{\text{ind}}^{\text{Sn}} = 0.006$  eV). Fits with constant bowing parameters for  $y < 0.06$  are shown as dotted lines in Fig. 2, and it is apparent that in the case of  $E_0$  such fit systematically underestimates the measured energies at Sn-concentrations beyond  $y = 0.07$ . Fitting the entire compositional range with a constant bowing expression yields  $b_0 = 2.24$  eV, well beyond the error of  $b_0$  as determined in Ref. 13. Thus, it appears that a constant bowing model is not accurate enough to explain the compositional dependence of the direct gap.

The simplest phenomenological extension of the constant bowing model is to assume the bowings to be linear functions of composition

$$b_0(y) = b_0^{(0)} + b_0^{(1)}y, \quad (3a)$$

$$b_{\text{ind}}(y) = b_{\text{ind}}^{(0)} + b_{\text{ind}}^{(1)}y. \quad (3b)$$

This assumption is more rigorously justified by the calculations described below. The use of Eq. (3a) implies that the compositional dependence of the band gap energy is given

by a cubic polynomial, which has been shown to apply in the case of  $\text{Ga}_{1-x}\text{Al}_x\text{As}$  (Ref. 1) and  $\text{Ga}_{1-x}\text{Al}_x\text{Sb}$  (Ref. 2). A cubic fit of the  $E_0$  energies gives  $b_0^{(0)} = 2.66 \pm 0.09$  eV and  $b_0^{(1)} = -5.4 \pm 1.1$  eV and is shown as a solid line in Figure 2. We see that it provides an excellent account of the experimental data. In addition, the expression implies  $E_0(0.14) = 0.40$  eV, in excellent agreement with the value  $E_0 = 0.41$  eV reported in Ref. 16 for a sample grown following a similar CVD approach. By contrast, if we use a constant bowing parameter  $b_0 = 2.46$  eV, as recommended in Ref. 13, the predicted value is  $E_0(0.14) = 0.33$  eV, which underestimates the experimental value.

The upper panels in Fig. 2 show the residuals from quadratic and cubic fits of the  $E_0$  energy. It is apparent that the quadratic residuals are larger and have a clear  $y$ -dependence. In fact, an  $F$ -test comparison of the two models gives  $F = 24.1$  for the 52 data points in the figure, which corresponds to a probability  $p < 1.5 \times 10^{-5}$  that the improved cubic fit is accidental. It is worth noting in this context that both quadratic and cubic fits were performed by assuming fixed end points. The question then arises as to whether the data could be equally well fit with a quadratic expression in which  $E_0^{\text{Sn}}$  is taken as an adjustable parameter, given the uncertainty of its room temperature value.<sup>13</sup> If we perform such a fit, however, we obtain the absurd value  $E_0^{\text{Sn}} = 7$  eV. Constraining  $E_0^{\text{Sn}}$  to a reasonable range produces inferior quadratic fits, and using cubic expressions in those cases lead to bowing parameters very similar to those quoted here using  $E_0^{\text{Sn}} = -0.413$  eV.

A critical consequence of the cubic fit is that the indirect to direct crossover composition is shifted to from  $y_c = 0.073$  to  $y_c = 0.090$ . However, this assumes that  $E_{\text{ind}}(y)$  is still given by a quadratic expression. Unfortunately, a fit of  $E_{\text{ind}}(y)$  using Eq. (3b) with no additional constraints gives unphysical results. This is mainly because the compositional range is too narrow, since  $E_{\text{ind}}$  cannot be clearly identified beyond  $y = 0.06$ . However, we can expect that the same physics that produces the compositional dependence of  $b_0$  will generate a similar effect for  $b_{\text{ind}}$ . The idea is then to combine the elementary theory in Eqs. (1) and (2) with experimental data to generate additional constraints that will make it possible to estimate  $b_{\text{ind}}^{(0)}$  and  $b_{\text{ind}}^{(1)}$ .

An important consideration when applying the theory in Eqs. (1) and (2) to  $\text{Ge}_{1-y}\text{Sn}_y$  alloys is the non-negligible increase in lattice parameter as a function of  $y$ . We note in this context that our definition of the function  $F(E,y)$  contains an explicit factor  $\Omega^{-2}(y)$  that does not appear in Ref. 15, where it is absorbed into the matrix element definition. In our case, however, we follow Hall and coworker<sup>17,18</sup> to define a matrix element  $M$  from which all possible dependencies on the unit cell volume have been extracted, so that we can extend Stroud's  $|M| = \text{constant}$  approximation to virtual crystals with different unit cell sizes. For the DOS, we start from the results of Chelikowsky and Cohen (CC) for Ge and  $\alpha$ -Sn.<sup>19</sup> The DOS regions near  $\Gamma_v$ ,  $L_c$ , and  $\Gamma_c$ , however, are modeled using accurate analytical expressions, which are joined smoothly with the CC DOS. The CB is described as the sum of three parabolic edges, corresponding to the  $L$ ,  $\Gamma$ , and  $\Delta$  minima, with  $k\cdot p$  effective masses from El Kurdi *et al.*<sup>20</sup> To this we added five Gaussians whose

amplitudes, energies, and widths were adjusted to match the CC DOS. The alloy DOS in the CB was simulated by linearly interpolating the  $L$ ,  $\Gamma$ , and  $\Delta$  edges, scaling the effective masses using  $k\cdot p$  theory, and interpolating the parameters of the five Gaussians. We use a similar approach for the VB, starting from the analytical results of Rodríguez-Bolívar *et al.*<sup>21</sup> for the region near  $\Gamma_v$ . An example of the DOS so computed is shown in Fig. 3 for the case of pure Ge ( $y = 0$ ). The function  $F(E,0)$  corresponding to this DOS is also shown in the figure. We note that, as expected,<sup>15</sup>  $F(0,0) > F(E_{\text{ind}},0)$ , so that  $b_{\text{ind}}^{(0)} > 0$ . We also find that  $F(0,0) > F(E_0,0)$ , which implies  $b_0^{(0)} > 0$ . Both results, which can be easily understood in terms of level repulsion, are consistent with the experimental data. Proceeding in this fashion we also computed  $F(E,y)$  and we find that for  $y < 0.2$  it is linear in  $y$  when evaluated at the energy of the  $\Gamma_v$ ,  $\Gamma_c$ , and  $L_c$  states at concentration  $y$ . Therefore, we can write

$$F(E,y) = F(E,0) + \left. \frac{dF(E,y)}{dy} \right|_{y=0} y. \quad (4)$$

Thus, the quantities  $F(E_0,0)$ ,  $F(E_{\text{ind}},0)$ , and  $F(0,0)$ , when inserted in Eq. (1), give  $b_0^{(0)}$  and  $b_{\text{ind}}^{(0)}$ , whereas if we insert  $dF(E_0,y)/dy$ ,  $dF(E_{\text{ind}},y)/dy$  and  $dF(0,y)/dy$  we obtain  $b_0^{(1)}$  and  $b_{\text{ind}}^{(1)}$ . The linearity in  $y$  of  $F(E,y)$  provides a more rigorous justification for the use of Eqs. (3a) and (3b). It remains approximately valid beyond  $y = 0.2$  and up to  $y = 0.66$ , where our DOS model ceases to be valid because  $E_0$  becomes negative. If we adjust  $|M|$  so that the calculated  $b_0^{(0)}$  agrees with the experimental value, we obtain  $b_{\text{ind}}^{(0)} = 2.14$  eV  $b_0^{(1)} = -4.4$  eV, and  $b_{\text{ind}}^{(1)} = -1.5$  eV.

Our theory predicts all signs in agreement with experiment, but the relative magnitude of the  $E_{\text{ind}}$  and  $E_0$  bowing would imply a much stronger compositional dependence of  $E_{\text{ind}}$  than observed experimentally. This is most likely a result of the crude constant matrix element approximation.

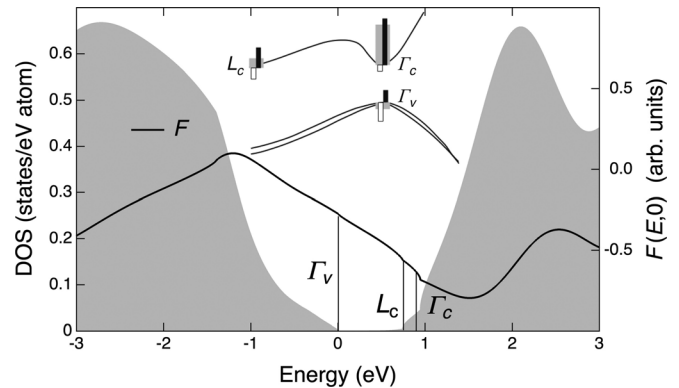


FIG. 3. The grey areas show the model electronic density of states for Ge over the energy range around the band gap. The solid line is the function  $F(E,0)$ , defined in Eq. (2). The bowing-induced shift of a state of energy  $E$  is proportional to this function. The inset shows the decomposition of the energy shifts induced by the parameters  $b_0^{(1)}$  and  $b_{\text{ind}}^{(1)}$  into contributions from individual states, displayed as thick grey bars drawn on a schematic band structure. In addition, for each state we show as thin black (white) bars the contribution to the shift from the interaction with the conduction (valence) band. In all cases, the shifts are positive when the bars are drawn upwards from the band structure, negative otherwise.



Clearly, matrix elements involving  $L_c$  need not be the same as those involving  $\Gamma_c$ . On the other hand, matrix elements between equivalent states appear in the expressions for  $b_0^{(0)}$  and  $b_0^{(1)}$ . We might then expect the ratio  $b_0^{(1)}/b_0^{(0)}$  to be less dependent on matrix elements, and indeed the theoretical value  $b_0^{(1)}/b_0^{(0)} = -1.65$  is in good agreement with the experimental result  $b_0^{(1)}/b_0^{(0)} = -2 \pm 1$ . If we assume the same to be valid for  $E_{\text{ind}}$ , we can fit the compositional dependence of this transition using Eq. (3b) subject to the constraint  $b_{\text{ind}}^{(1)}/b_{\text{ind}}^{(0)} = -0.7$  that we obtain from our theoretical model. We find  $b_{\text{ind}}^{(0)} = 1.11 \pm 0.07$  eV and  $b_{\text{ind}}^{(1)} = -0.78 \pm 0.07$  eV. The corresponding curve is shown as a solid line in Fig. 2, and we see that it intercepts the  $E_0$  line at  $y_c = 0.087$ . Thus, the predicted cross-over composition from indirect to direct gap behavior in  $\text{Ge}_{1-y}\text{Sn}_y$  alloys is increased by more than 1% relative to earlier work that ignored the compositional dependence of the bowing parameters.<sup>13</sup>

The theoretical value  $b_{\text{ind}}^{(1)}/b_{\text{ind}}^{(0)} = -0.7$ , as opposed to  $b_0^{(1)}/b_0^{(0)} = -1.65$ , implies that the difference between cubic and quadratic fits are more pronounced for  $E_0$ , as is apparent in Fig. 2. To understand this difference, we write  $b_0^{(1)} = [b_{\Gamma_{c,c}}^{(1)} + b_{\Gamma_{c,v}}^{(1)}] - [b_{\Gamma_{v,v}}^{(1)} + b_{\Gamma_{v,c}}^{(1)}]$  and  $b_{\text{ind}}^{(1)} = [b_{L_{c,c}}^{(1)} + b_{L_{c,cv}}^{(1)}] - [b_{\Gamma_{v,v}}^{(1)} + b_{\Gamma_{v,c}}^{(1)}]$ , where each of the square brackets corresponds to a state involved in the transition, and the contribution from each state is split into two terms (subscripts  $c$  and  $v$ ) corresponding to splitting the DOS in Eq. (2) into VB and CB terms. The inset of Fig. 3 shows the energy shifts associated with these different contributions. The thick grey bars represent the shift of each state, and the thin black and white bars its decomposition into CB and VB contributions, respectively. We notice that both gaps are *increasing*. This illustrates the fact that  $b_0^{(1)}$  and  $b_{\text{ind}}^{(1)}$  are found to be *negative*. However, the effect is much larger for  $E_0$ , and this is mainly associated with the positive shift caused by the interaction of  $\Gamma_c$  with the CB (thin black bar), which almost doubles the corresponding  $L_c$  shift. This can be traced back to the fact that  $\Gamma_c$  is only 55 meV below the  $\Delta_c$  minimum of the  $\Delta$ -related DOS. By contrast, the separation between  $\Delta_c$  and  $L_c$  is 200 meV, so that the repulsion is weaker. The  $\Delta_c$  state is found at similar energies in Si, Ge, and  $\alpha$ -Sn, which implies that its compositional dependence is weak. On the other hand,  $\Gamma_c$  in the virtual crystal shifts rapidly down as a function of  $y$ , *increasing* its separation from  $\Delta_c$  and therefore *reducing* the level repulsion. This is represented by a *positive* large bar in the inset of Fig. 3, or, equivalently, by a large, *negative*  $b_{\Gamma_{c,c}}^{(1)}$  coefficient. By contrast, in the case of  $L_c$  the level repulsion change is greatly diminished because the initial separation at  $y = 0$  is already relatively large, and also because  $L_c$  moves down more slowly than  $\Gamma_c$  as a function of  $y$ . Thus, the corresponding black bar is much smaller, which means  $|b_{L_{c,c}}^{(1)}| < |b_{\Gamma_{c,c}}^{(1)}|$ . Since these derivative-like subtleties in the Ge DOS have a strong impact on the value of  $b_0^{(1)}$  and  $b_{\text{ind}}^{(1)}$ , it is not surprising that supercell calculations using different band structure methods make wildly different predictions, ranging from  $b_0^{(1)} = -5.6$  eV (Ref. 22) to

$b_0^{(1)} = -0.9$  eV.<sup>23</sup> It is now possible to speculate on the reason why  $|b_0^{(0)}| > 2|b_{\text{ind}}^{(0)}|$ , whereas our theory predicts  $|b_0^{(0)}| \sim |b_{\text{ind}}^{(0)}|$ . It is apparent from Fig. 3 that the separation between  $L_c$  and  $\Gamma_c$  is too small to obtain a large difference in bowing parameters for  $E_0$  and  $E_{\text{ind}}$  using constant matrix elements. However, if the coupling with the  $\Delta$ -DOS is stronger than with other states, it is conceivable that a large difference in bowing parameters might result even for these closely lying states.

In summary, we have presented experimental evidence for the compositional dependence of the bowing parameter for  $E_0$  in  $\text{Ge}_{1-y}\text{Sn}_y$  alloys. A fit to the experimental data gives (in eV)  $b_0(y) = 2.66 - 5.4 y$ . We then use a simple theoretical model of the band gap bowing to conclude that the compositional dependence of  $b_{\text{ind}}$  should be weaker than the one observed for  $b_0$ . Using the predictions from this model, we estimate a crossover concentration of  $y_c = 0.087$ , significantly increased from earlier estimates based on a strictly quadratic compositional dependence of the band gaps. The discontinuous reversal of band curvatures when the direct gap becomes negative makes it unlikely that Eqs. (3a) and (3b) will remain valid over the entire compositional range from pure Ge to pure  $\alpha$ -Sn. Thus our prediction  $b_0(1) = -2.7$  eV could deviate substantially—even in sign—from the bowing parameter for Sn-rich  $\text{Ge}_{1-y}\text{Sn}_y$  alloys. In the case of indirect gap, we predict  $b_{\text{ind}}(1) = 0.33$  eV. This gap has been measured near the Sn-end.<sup>24</sup> Only a few data points are available and the data are noisy, but a fit gives a substantially larger  $b_{\text{ind}}(1) = 1.3$  eV, confirming the perils of extrapolating our results. Detailed measurements near the Sn-rich end are needed, and the result is likely to be that even cubic polynomials are insufficient to describe the compositional dependence of band gaps in  $\text{Ge}_{1-y}\text{Sn}_y$  alloys over the entire compositional range.

Illuminating discussions with P. Batson and A. V. G. Chizmeshya are gratefully acknowledged. This work was funded and supported by the Air Force Office of Scientific Research under Contract Nos. DOD AFOSR FA9550-12-1-0208 and DOD AFOSR FA9550-13-1-0022.

<sup>1</sup>D. E. Aspnes, S. M. Kelso, R. A. Logan, and R. Bhat, *J. Appl. Phys.* **60**(2), 754 (1986).

<sup>2</sup>V. Bellani, M. Geddo, G. Guizzetti, S. Franchi, and R. Magnanini, *Phys. Rev. B* **59**(19), 12272 (1999).

<sup>3</sup>I. Vurgaftman, J. R. Meyer, and L. R. Ram-Mohan, *J. Appl. Phys.* **89**(11), 5815 (2001).

<sup>4</sup>I. Vurgaftman and J. R. Meyer, *J. Appl. Phys.* **94**(6), 3675 (2003).

<sup>5</sup>S. H. Wei and A. Zunger, *Phys. Rev. Lett.* **76**(4), 664 (1996).

<sup>6</sup>L. Bellaiche, S.-H. Wei, and Z. Zunger, *Phys. Rev. B* **54**(24), 17568 (1996).

<sup>7</sup>W. Shan, W. Walukiewicz, J. W. Ager, E. E. Haller, J. F. Geisz, D. J. Friedman, J. M. Olson, and S. R. Kurtz, *Phys. Rev. Lett.* **82**(6), 1221 (1999).

<sup>8</sup>T. Mattila, S.-H. Wei, and A. Zunger, *Phys. Rev. B* **60**(16), R11245 (1999).

<sup>9</sup>V. R. D'Costa, C. S. Cook, A. G. Birdwell, C. L. Littler, M. Canonico, S. Zollner, J. Kouvetakis, and J. Menendez, *Phys. Rev. B* **73**(12), 125207 (2006).

<sup>10</sup>D. W. Jenkins and J. D. Dow, *Phys. Rev. B* **36**(15), 7994 (1987).

<sup>11</sup>K. A. Mäder, A. Baldereschi, and H. von Kanel, *Solid State Commun.* **69**(12), 1123 (1989).

- <sup>12</sup>C. I. Ventura, J. D. Querales Flores, J. D. Fuhr, and R. A. Barrio, "Electronic structure of  $\text{Ge}_{1-x-y}\text{Si}_x\text{Sn}_y$  ternary alloys for multijunction solar cells," *Prog. Photovoltaics: Res. Appl.* (published online 2013).
- <sup>13</sup>L. Jiang, J. D. Gallagher, C. L. Senaratne, T. Aoki, J. Mathews, J. Kouvetakis, and J. Menéndez, *Semicond. Sci. Technol.* **29**, 115028 (2014).
- <sup>14</sup>C. L. Senaratne, J. D. Gallagher, L. Jiang, T. Aoki, D. J. Smith, J. Menéndez, and J. Kouvetakis, *J. Appl. Phys.* **116**, 133509 (2014).
- <sup>15</sup>D. Stroud, *Phys. Rev. B* **5**(8), 3366 (1972).
- <sup>16</sup>M. R. Bauer, J. Tolle, C. Bungay, A. V. G. Chizmeshya, D. J. Smith, J. Menendez, and J. Kouvetakis, *Solid State Commun.* **127**(5), 355 (2003).
- <sup>17</sup>G. Hall, *Phys. Rev.* **116**(3), 604 (1959).
- <sup>18</sup>A. Asch and G. Hall, *Phys. Rev.* **132**(3), 1047 (1963).
- <sup>19</sup>J. R. Chelikowsky and M. L. Cohen, *Phys. Rev. B* **14**(2), 556 (1976).
- <sup>20</sup>M. El Kurdi, G. Fishman, S. B. Sauvage, and P. Boucaud, *J. Appl. Phys.* **107**(1), 013710 (2010).
- <sup>21</sup>S. Rodríguez-Bolívar, F. M. Gómez-Campos, and J. E. Carceller, *Semicond. Sci. Technol.* **20**(1), 16 (2005).
- <sup>22</sup>Y. Chibane and M. Ferhat, *J. Appl. Phys.* **107**, 053512 (2010).
- <sup>23</sup>W.-J. Yin, X.-G. Gong, and S.-H. Wei, *Phys. Rev. B* **78**(16), 161203 (2008).
- <sup>24</sup>C. Hoffman, J. Meyer, R. Wagner, F. Bartoli, M. Engelhardt, and H. Höchst, *Phys. Rev. B* **40**(17), 11693 (1989).